https://doi.org/10.5194/egusphere-2026-2588
Preprint. Discussion started: 20 May 2026

Multidecadal North Atlantic Circulation Shifts under Historical Anthropogenic Forcing in CESM2-LE

Ina Nagler[1], Helene Asbjørnsen[2], and Andreas Born[1]

[1]Department of Earth Sciences, University of Bergen, and Bjerknes Centre for Climate Research, Allégaten 41, 5007 Bergen, Norway
[2]Geophysical Institute, University of Bergen, and Bjerknes Centre for Climate Research, Allégaten 70, 5007 Bergen, Norway

Correspondence: Ina Nagler (ina.nagler@uib.no)

Abstract. The North Atlantic subpolar gyre is a critical region for global climate, yet the mechanisms driving its multidecadal circulation variability under anthropogenic forcing remain poorly understood. This study investigates the physical processes underlying large multidecadal shifts in density overturning strength at 55°N using a 100-member ensemble of the Community Earth System Model version 2 (CESM2). Using change point and composite analyses, we identify three distinct categories of circulation shifts: strengthening events, and two types of weakening events separated by a 1985 regime shift. Strengthening shifts are driven by an internal positive feedback where enhanced surface heat loss triggers deep convection and strengthened horizontal gyre circulation, subsequently increasing northward heat and salt transport that sustains the anomaly. Weakening shifts before 1985 are primarily driven by internal density-gradient adjustments between the subpolar and subtropical gyres. In contrast, post-1985 weakening events are characterized by basin-wide thermodynamic changes, where greenhouse gas-induced warming and reduced surface buoyancy loss suppress convection across the Irminger Sea and eastern subpolar North Atlantic. Our results reveal that these shifts are non-linear and asymmetric, reflecting a transition from a salinity-dominated internal variability regime to a forced, temperature-driven regime. These findings suggest that the North Atlantic circulation is undergoing a fundamental change in its governing dynamics, highlighting the increasing influence of anthropogenic forcing on the stability of the Atlantic Meridional Overturning Circulation.

1 Introduction

Anthropogenic forcing alters the dynamics of the Earth's climate system, complicating our interpretation of climate variability (Rodgers et al., 2021). This challenge is particularly pertinent to the Atlantic Ocean circulation, where continuous observations of overturning strength since 2004 are insufficient for evaluating long-term trends (Latif et al., 2022). The Atlantic Meridional Overturning Circulation (AMOC) displays variability from interannual to multidecadal and centennial timescales, thereby complicating the assessment of human-induced changes (Lozier, 2010; Zhang et al., 2019; Moat et al., 2024). Alterations in the AMOC have the potential to lead to significant global consequences, affecting ocean heat content, anthropogenic carbon uptake, climate sensitivity, and dynamic sea level changes (Fox-Kemper et al., 2021). Calvin et al. (2023) report that it is very likely the AMOC will decline in the 21st century, but the magnitude is highly uncertain, in part due to our limited understanding of how anthropogenic forcing interacts with multidecadal AMOC variability.

https://doi.org/10.5194/egusphere-2026-2588
Preprint. Discussion started: 20 May 2026

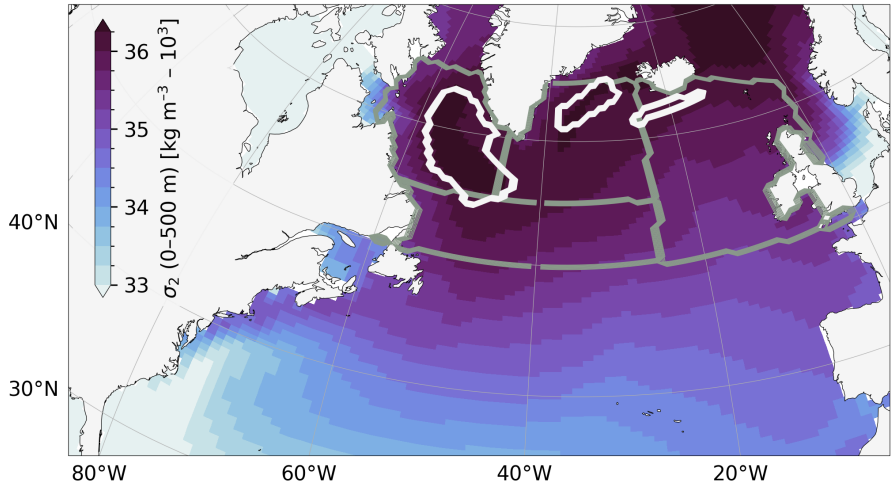

Figure 1. Ensemble-mean 0–500 m potential density (σ_2) over the period 1850–1860. The white contours show the regions used to evaluate mixed-layer depth in the convection centres, defined as the area where the time-mean of the annual maximum mixed-layer depth in the CESM2 piControl simulation exceeds 1000 m. The subpolar North Atlantic (SPNA) region, shown by the grey lines, is defined as 45°–65°N and 70° W to 0°. The SPNA is additionally divided into four sub-regions: the Eastern SPNA, the Irminger Sea, the Labrador Sea, and the Central SPNA.

Understanding the mechanisms behind climate variability on multidecadal timescales is essential for making accurate predictions (Yeager and Robson, 2017). Coupled Earth system models exhibit multidecadal variability in the AMOC with differing periods among models (Danabasoglu, 2008), which has prompted extensive investigations into the mechanisms underlying this variability (Zhang et al., 2019). Observational data reveal signals of decadal to multidecadal variability across multiple variables in the North Atlantic climate system (Robson et al., 2018). However, there is no clear consensus on the drivers of this variability (Moat et al., 2024). Various mechanisms have been summarised by Zhang et al. (2019), with many studies suggesting the role of the AMOC as a primary driver, while some propose a dynamical coupling between atmospheric and oceanic circulations (e.g. Sutton et al., 2018). A decade ago, the link between Labrador Sea Water formation and the AMOC was regarded as a deciding factor in North Atlantic variability (Eden and Willebrand, 2001; Zhang, 2010; Yeager and Danabasoglu, 2014; Kwon and Frankignoul, 2014). However, recent findings have raised questions about the validity of this relationship (Lozier et al., 2019). Despite these uncertainties, the subpolar gyre (SPG) has been identified as the key region influencing multidecadal variability in the North Atlantic (Wills et al., 2019).

The SPG is an important region for AMOC variability due to the complex interactions between the horizontal circulation, deep water formation, and sea ice processes (Kostov et al., 2021; Lozier, 2023). Figure 1 shows the upper 500 meter potential density in the North Atlantic, demonstrating that upper ocean isopycnals do not align with latitudes, particularly in the subpolar North Atlantic (SPNA). This misalignment is a result of substantial heat loss along the upper pathways of the AMOC and the SPG (Lozier et al., 2019). Berglund et al. (2023) describe how subtropical surface water circulates in the subtropical gyre

https://doi.org/10.5194/egusphere-2026-2588
Preprint. Discussion started: 20 May 2026

(STG), where it loses heat and salt. It then continues north in the North Atlantic Current, mixing with subpolar waters, which leads to further heat loss and freshening, thereby increasing the density (e.g. Asbjørnsen et al., 2021). When it reaches the subpolar gyre region, sufficiently dense water forms through surface-forced watermass transformation and mixing with dense water formed in the Nordic Seas (Dey et al., 2024; Evans et al., 2023) to sink and return southward at depth (Rhein et al., 2015). These complex dynamics generate variability across the spectrum of temporal scales, necessitating the use of Earth system models to facilitate investigations of the climate system in the past and projections of future climates.

The multidecadal variability of the AMOC is closely connected to the propagation of density anomalies (Eden and Willebrand, 2001; Lohmann et al., 2009; Tulloch and Marshall, 2012; Yeager et al., 2021). While analyses of changes in heat content (Moat et al., 2019; Robson et al., 2012; Zhang and Zhang, 2015) and freshwater content (Dickson et al., 1988; Holliday et al., 2020) are often used to identify the physical drivers of circulation changes, it is ultimately density that governs the movement of water masses, making it the most physically relevant metric. Evaluating overturning in density space provides insights into changes in water mass transformation (Kwon and Frankignoul, 2014), one of the essential processes that drive the overturning circulation. Increasingly, studies are examining how density anomalies propagate within the SPG (Zhang, 2010; Kwon and Frankignoul, 2014; Menary et al., 2020; Lai et al., 2022; Zhu et al., 2023). However, there remains a lack of quantitative information on the propagation of these density anomalies and their multidecadal variability during the historical period (Bellomo et al., 2018).

In this study, we investigate the primary mechanisms behind large multidecadal shifts in circulation in the SPNA, detail which processes are most influential and how they operate in a 100-member ensemble from a coupled Earth system model, allowing for a consistent consideration of natural variability during the historical period while focusing on underlying physical processes within a single model system. We identify multidecadal circulation shifts via change point analysis and investigate their common dynamics through composite analysis. Our findings identify one type of increase and two types of decrease shifts in density overturning transport, highlighting the key factors contributing to these changes and the propagation of density anomalies to depth. These findings imply that North Atlantic variability is governed by non-linear, asymmetric responses to external forcing, and that the model ensemble shows a distinct post-1985 SPG regime compared with the pre-1985 period.

2 Methodology

In this study we use the CESM2 Large Ensemble (CESM2-LE), encompassing a 100-member ensemble of a fully coupled Earth system model with a nominal 1° horizontal resolution across all components. The ocean model component, the Parallel Ocean Program version 2 (POP2), includes 60 vertical levels, with 20 layers within the upper 200 meters (Rodgers et al., 2021). Improved model physics in CESM2 result in a refined representation of the Earth system when comparing CESM1 and CESM2 against observational data. For instance, the depth overturning strength is reduced by approximately 2 Sv relative to CESM1, but both model versions exceed observational estimates at 26.5° N (Danabasoglu et al., 2020). CESM2-LE is forced by CMIP6 historical radiative scenarios (1850–2014) and SSP3-7.0 (2015–2100). Half the ensemble follows the standard CMIP6 protocol; the remainder applies smoothed biomass burning fluxes to reduce discontinuities during 1990–2020. The ensemble spread is

https://doi.org/10.5194/egusphere-2026-2588
Preprint. Discussion started: 20 May 2026

created from combinations of oceanic and atmospheric initial states, including macro initialisations spaced every 10 years between years 1001–1191 of the piControl simulation, and 80 micro initialisations from four piControl years representing distinct AMOC phases. Micro-initialised members are not independent immediately post-1850; the ensemble-mean AMOC for micro-perturbation clusters only diverges into distinct trajectories after several decades (Rodgers et al., 2021).

A common approach to characterising the large-scale North Atlantic circulation, a four-dimensional system (time, longitude, latitude, depth or density), involves reducing the data by one dimension through the computation of streamfunctions, followed by further reduction through analysing the streamfunction maximum at specific locations to produce time series of transport strength. The overturning streamfunction in potential density space, $\psi_\sigma(t, y, \sigma')$, is defined as

$$\psi_\sigma(t) = \int_{\sigma_{\min}}^{\sigma_{\max}} \int_{x_{\text{west}}}^{x_{\text{east}}} v(t, x, y, \sigma')\, dx\, d\sigma', \tag{1}$$

and computed by summing the meridional velocities zonally and accumulating over density classes. Potential density referenced to a pressure of 2000 dbar is employed, consistent with standard practice for density-space overturning streamfunctions (Oliveira Matos et al., 2025). The overturning streamfunction in depth-space, $\psi_d(t)$, is defined as

$$\psi_d(t) = \int_{z_{\text{bottom}}}^{z_{\text{surface}}} \int_{x_{\text{west}}}^{x_{\text{east}}} v(t, x, y, z')\, dx\, dz', \tag{2}$$

and computed by summing meridional velocities zonally and vertically accumulating from surface to bottom. The barotropic streamfunction, $\psi_b(t)$, is defined as

$$\psi_b(t) = \int_{x_{\text{west}}}^{x_{\text{east}}} \int_{z_{\text{bottom}}}^{z_{\text{surface}}} v(t, x', y, z)\, dz\, dx', \tag{3}$$

and computed by vertically summing meridional velocity and zonally accumulating from west to east.

We investigate variability in the subpolar overturning strength by taking the maximum of the annual mean overturning strength at 55° N, $\psi_\sigma^{\max(55^\circ\,\text{N})}(t)$ for each ensemble member. The resulting time series exhibit an ensemble spread of approximately 5 Sv in the annual mean (Fig. 2a). Change point analysis is applied to detect significant shifts in circulation strength. This method identifies changes in the statistical properties of a time series, indicating transitions in underlying processes (Truong et al., 2020). A shift is defined as occurring when the 20-year mean exceeds or falls below the mean of the preceding 40 years by more than three times the standard deviation of that 40-year period (Fig. 2a; 3σ threshold). We additionally reduce the detection threshold to two and one standard deviation (2σ and 1σ; Fig. 2b) to also explore circulation shifts of smaller magnitudes.

We employ composite analysis to identify common mechanisms underlying overturning strength changes (Truong et al., 2020). The detected shifts are classified into three categories: increases in overturning strength around 1895 and 1955, and decreases near 1925 and from the 1970s onwards. The robustness of the categories was confirmed through sensitivity analyses varying grouping structure and temporal thresholds. For each category, we calculate composite sequences for the 40 years preceding and 20 years following the shift identified by the change point analysis.

https://doi.org/10.5194/egusphere-2026-2588
Preprint. Discussion started: 20 May 2026

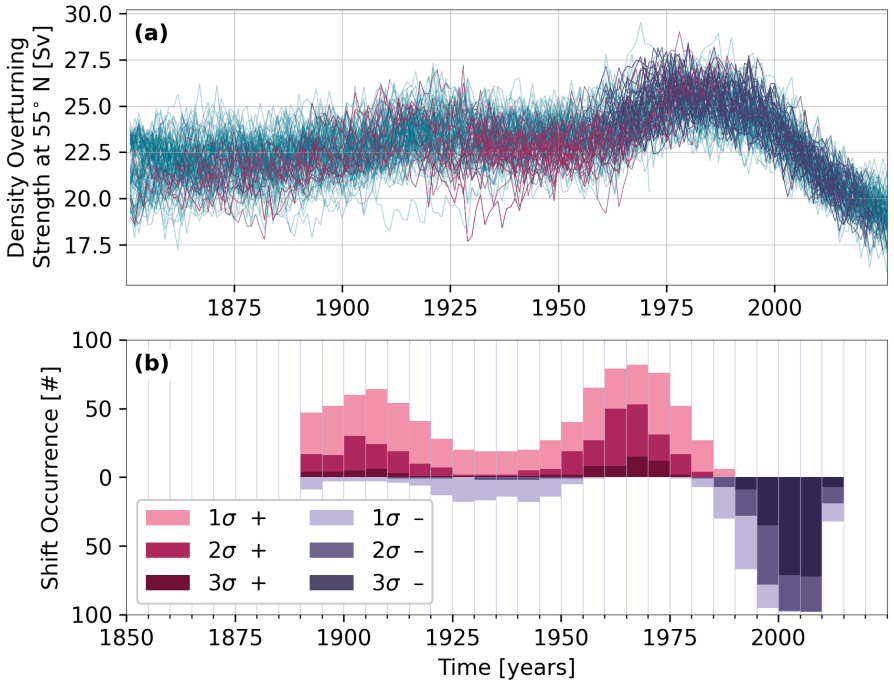

Figure 2. (a) Time series of overturning strength in density space at 55°N, $\Delta\psi_{\sigma}^{\max}(55^{\circ}\mathrm{N})$, where each line represents an individual ensemble member from 1850–2030. The 3σ increase and decrease shifts are marked in pink and purple respectively. **(b)** Occurrence of circulation shifts identified by the change point analysis at the 1σ, 2σ, and 3σ levels. Pink bars indicate the number of strengthening events and purple bars indicate the number of weakening events.

We analyse hydrographic variables that characterise key physical processes, focusing on winter conditions when atmospheric forcing is strongest and oceanic responses are most pronounced. The winter mean includes March, as the climatological mixed layer depth in the Labrador Sea peaks during this month (Gu et al., 2024). The selected variables are those found to play an important role in the processes described in this study: salinity, temperature, potential density referenced to a pressure of 2000 dbar, mixed layer depth (as an indicator of convective activity), surface heat loss, and northward heat transport. Additional variables, including sea ice area, surface wind stress, sea level pressure, sea surface height, and northward salt transport, were examined but did not provide further insight for the present analysis.

The spatial and temporal evolution of the composites is examined using sequential anomaly maps. We calculate anomalies relative to the mean of the 40 years preceding each shift. The barotropic streamfunction and mixed-layer depth are shown as model-output fields, with temperature, salinity, and potential density averaged over the upper 500 m. To capture density changes through the full water column, four regions are defined (Fig. 1) and regional averages are computed to track their evolution over time and depth.

https://doi.org/10.5194/egusphere-2026-2588
Preprint. Discussion started: 20 May 2026

We compute time series for circulation and hydrographic metrics, normalised by subtracting the mean of the first 40 years and dividing by the corresponding standard deviation. The metrics are: the maximum of the overturning streamfunction in density space at 55° N, $\psi_{\sigma}^{\max}(55^{\circ}\,\mathrm{N})$; the minimum of the barotropic streamfunction within the SPNA box (45°–65° N, 70° W to 0°), $\psi_{b}^{\min}(\mathrm{SPNA})$; the maximum of the overturning streamfunction in depth space at 26° N, $\psi_{d}^{\max}(26^{\circ}\,\mathrm{N})$; the northward heat transport at 45°, $\mathrm{Nheat}(45^{\circ}\,\mathrm{N})$; the mixed layer depth in convection centres defined from the pre-industrial control run, $\mathrm{MLD(conv)}$; surface heat flux within the SPNA box, $Q_{\mathrm{surf}}(\mathrm{SPNA})$; and the potential density, together with its salinity and temperature contributions obtained by holding temperature or salinity fixed at their mean over the first 40 years of the shift (calculated over the entire record for Fig. 11), all integrated over the full water column in the SPNA box, $\sigma(\mathrm{SPNA})$, $\sigma_{\mathrm{salt}}(\mathrm{SPNA})$, and $\sigma_{\mathrm{temp}}(\mathrm{SPNA})$.

3 Results

We identify three categories of multidecadal circulation shifts: strengthening shifts (77 cases, 3 σ), pre–1985 weakening shifts (12 cases, 2 σ), and post–1985 weakening shifts (195 cases, 3 σ). When the threshold is lowered to 2 σ, we identify pre–1985 weakening shifts that are absent at the 3 σ criterion and that develop through mechanisms distinct from those driving the post–1985 weakening shifts. While every ensemble member experiences at least one 3 σ weakening after 1985, the timing of these events varies among members. Figure 2b shows the timing of the 3 σ, 2 σ, and 1 σ shifts, revealing a pattern consistent with AMOC changes reported in several studies (e.g. Menary et al., 2020).

In the following, we examine composites for each category of circulation shift separately: 3 σ strengthening, 2 σ weakening before 1985, and 3 σ weakening after 1985. We first outline the patterns evident in the composites, then highlight the differences between the three categories. For strengthening and post–1985 weakening shifts, the composites show at least four decades of relatively stable overturning before onset, which reflects the averaging over differing pre-shift states across members rather than necessarily indicating a persistent condition in every case. In contrast, pre–1985 weakening composites display earlier hydrographic and circulation changes that appear to set up the subsequent decline. The mechanisms associated with each category are described in the following subsections.

3.1 Shifts towards increased overturning

During the ‘increase shifts’ we observe an initial cooling of the upper 500 m (Figs. 3d and e). This cooling coincides with the onset of increased surface heat loss (Fig. 4b and c) and, simultaneously, with a rise in the density of the upper-ocean layers, especially in the eastern and central subpolar North Atlantic (SPNA) (Fig. 5a–d). The increase in density reduces stratification, thereby enhancing deep convection, which drives a baroclinic flow of relatively light water around the dense centre (Born et al., 2013). This strengthening of horizontal circulation in the SPG is illustrated in Fig. 3b and c, and Fig. 4a. As horizontal transport intensifies, density overturning in the SPG increases, a trend illustrated in Fig. 4a, which can manifest as either enhanced formation of dense water or increased meridional velocities.

https://doi.org/10.5194/egusphere-2026-2588
Preprint. Discussion started: 20 May 2026

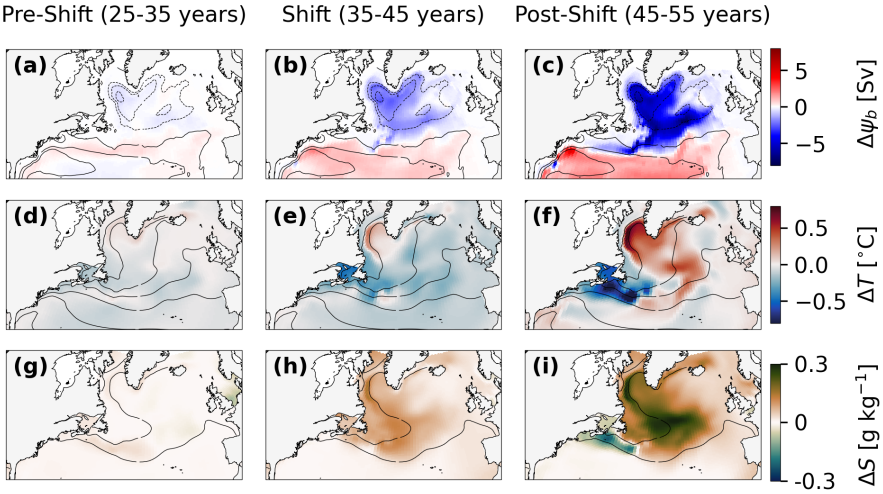

Figure 3. Ten-year averaged composite anomalies associated with 3σ increase shifts in density overturning strength at 55°N. Rows show anomalies in: **(a–c)** barotropic streamfunction ($\Delta\Psi_b$), **(d–f)** upper 500 m temperature (ΔT), and **(g–i)** upper 500 m salinity (ΔS). Columns represent: pre-shift (year 25–35; left), shift (year 35–45; centre), and post-shift (year 45–55; right).

The strengthened overturning circulation transports density anomalies to deeper layers and carries subtropical waters northward into the SPG (Fig 4b), which introduces additional heat and salinity. The additional heat transported into the SPG is offset by an increase in surface heat loss, as reported by Robson et al. (2022). Consequently, no immediate warming occurs; instead, the rise in salinity sustains an increase in density (Fig. 3h and i, and Fig. 4c). This sustained increase in primarily surface density, in turn, reinforces the overturning circulation, creating a positive feedback loop (Fig. 5a).

As described in Section 2, the SPNA is divided into four regions (Fig. 1); we then examine the evolution of density anomalies in depth–time space (Fig. 5a–d). In the eastern SPNA, a pronounced surface signal is observed before the onset of the increase in overturning. This surface signal is then transported to greater depths in the Irminger and Labrador Seas, where the convection centres lie, and this density anomaly re-emerges at depth in the eastern SPNA, signalling recirculation. This leads to the SPG expanding southward, which can be seen in the horizontal transport in Fig. 3c and the strong density anomaly in the central SPG box in Fig. 5a–d.

The stabilisation of density overturning within the SPG is governed by the interplay of surface heat flux and salinity. Five years after the change point, surface heat loss stops increasing and no longer offsets higher northward heat transport (Fig. 4a and b). At this stage the density ceases to rise, even though the SPG continues to become saltier, as the increase in salinity is offset by the additional heat. The magnitude of the density anomaly remains at around five times the standard deviation of the first 40 years of the composite period until year 55, when temperature begins to dominate density, leading to a decrease in density (Fig. 4c and Fig. 5a–d). As a result, convection begins to decrease, and the strength of the circulation no longer increases (Fig. 4a and b).

https://doi.org/10.5194/egusphere-2026-2588
Preprint. Discussion started: 20 May 2026

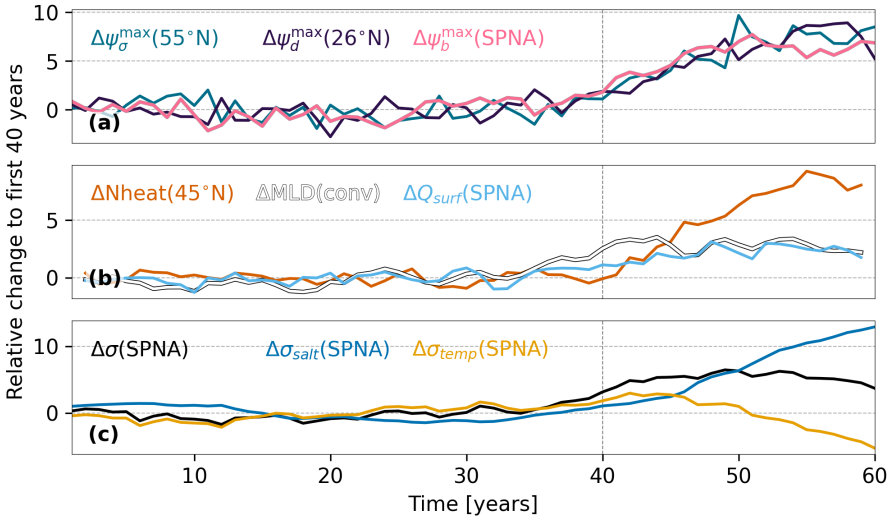

Figure 4. Composite anomalies relative to the mean of the first 40 years of the composite period, associated with the 3σ increase shift in density overturning strength at 55°N. The vertical grey dashed line marks the timing of the shift. **(a)** Top panel: density overturning strength at 55°N ($\Delta\psi_\sigma^{\max}(55°\mathrm{N})$; green), depth overturning strength at 26°N ($\Delta\psi_d^{\max}(26°\mathrm{N})$; black), and maximum horizontal transport in the SPNA ($\Delta\psi_b^{\min}(\mathrm{SPNA})$; pink). **(b)** Middle panel: northward heat transport at 45°N ($\Delta\mathrm{Nheat}(45°\mathrm{N})$; red), mean mixed-layer depth in the PiControl convection centres ($\mathrm{MLD}(conv)$; white), and SPNA-averaged surface heat flux ($\Delta Q_{surf}(\mathrm{SPNA})$; light blue). **(c)** Bottom panel: SPNA density ($\Delta\sigma(\mathrm{SPNA})$; black), thermal contribution to density ($\Delta\sigma_{temp}(\mathrm{SPNA})$; yellow), and haline contribution to density ($\Delta\sigma_{salt}(\mathrm{SPNA})$; blue). SPNA is defined in Fig. 1

3.2 Pre–1985 shifts towards decreased overturning

Shifts in density overturning prior to 1985 are smaller in magnitude, remaining below three standard deviations, and produce less pronounced effects than those in later years. The composite anomaly map for years 25–35 (Fig. 6d) shows upper-ocean warming across the SPG, cooling in the northern subtropical gyre (STG), and warming in the southern STG, providing the broader context for the period. Central to this pre-shift interval is a progressive, temperature-driven decrease in density within the SPG, evident in the full 40-year pre-shift composite record shown in Fig. 7c. This regional warming decreases upper-ocean density, thereby reducing vertical mixing (Fig. 5e–h) and weakening horizontal gyre transport (Fig. 6b). This process aligns with findings that a decay of the domed isopycnal structure in the SPG diminishes the gyre's strength (Lohmann et al., 2009).

The temperature and salinity anomalies associated with pre–1985 decrease shifts lead to reduced meridional density gradients between the subtropical and subpolar latitudes during and after the shift. A weakening of the meridional density gradient has previously been associated with a reduction in the AMOC and northward heat transport (Sévellec and Huck, 2015). This is consistent with the gradual decline of northward heat transport seen in Fig. 7b. Te Raa and Dijkstra (2002) showed that, on interdecadal timescales, a positive meridional temperature-gradient anomaly between the gyres induces a negative meridional overturning anomaly. Consistently, depth overturning at 26° N begins to weaken around year 35. At the same time, buoyant

https://doi.org/10.5194/egusphere-2026-2588
Preprint. Discussion started: 20 May 2026

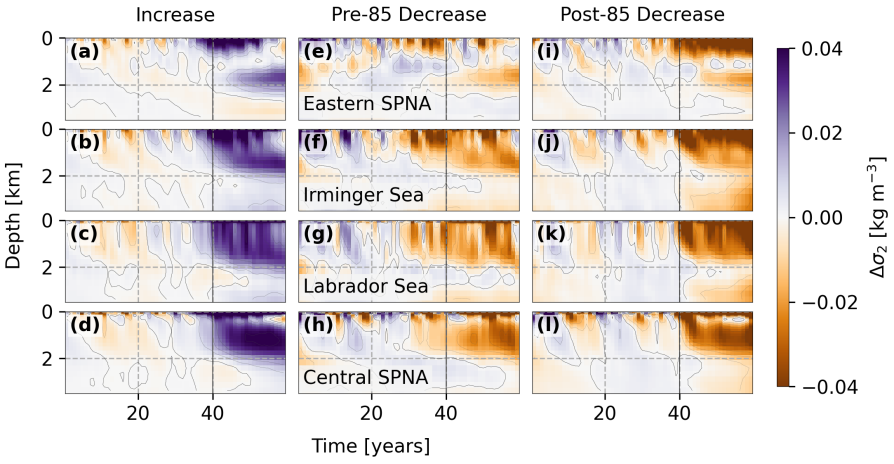

Figure 5. Temporal evolution of potential density anomalies ($\Delta\sigma_2$) averaged within the four sub-regions defined in Fig. 1. Composite annual $\Delta\sigma_2$ from 0 to 3.5 km depth is presented. Columns represent: increase shifts **(a–d)**, pre-1985 decreases **(e–h)**, and post-1985 decreases **(i–l)**. Within each column, rows show (from top to bottom) the Eastern SPNA, Irminger Sea, Labrador Sea, and Central SPNA.

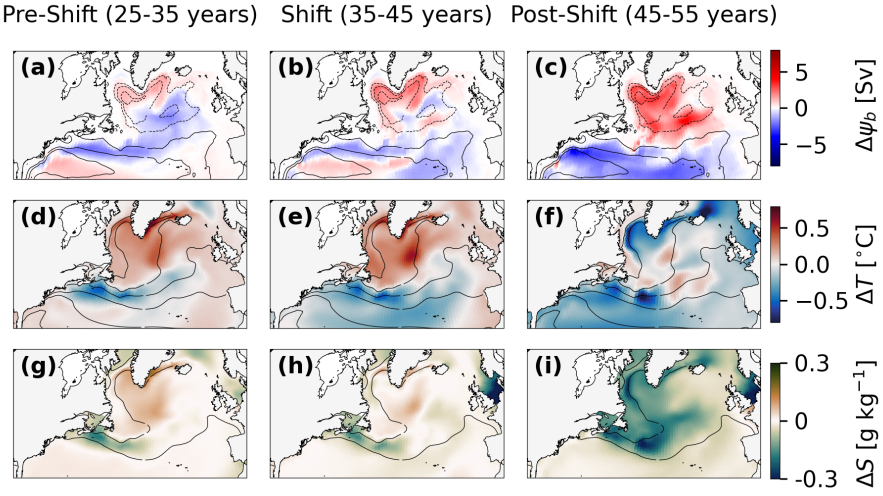

Figure 6. Same as Fig. 3 but here for 2σ decrease shifts before 1985.

anomalies reach 1000 m depth throughout the SPNA, and the composite period exhibits its strongest density reductions in the Irminger Sea before year 40 (Fig. 5e–h).

The reduced heat transport across 45°N, likely related to reduced inter-gyre transport, causes the SPG to freshen and cool (Fig. 6d–i and Fig. 7c). This freshening dominates the SPNA's density, alters regional stratification, thereby reducing gyre strength and consequently diminishing density overturning (Fig. 5e–h and Fig. 7a). By year 45 the gyre circulation and asso-

https://doi.org/10.5194/egusphere-2026-2588
Preprint. Discussion started: 20 May 2026

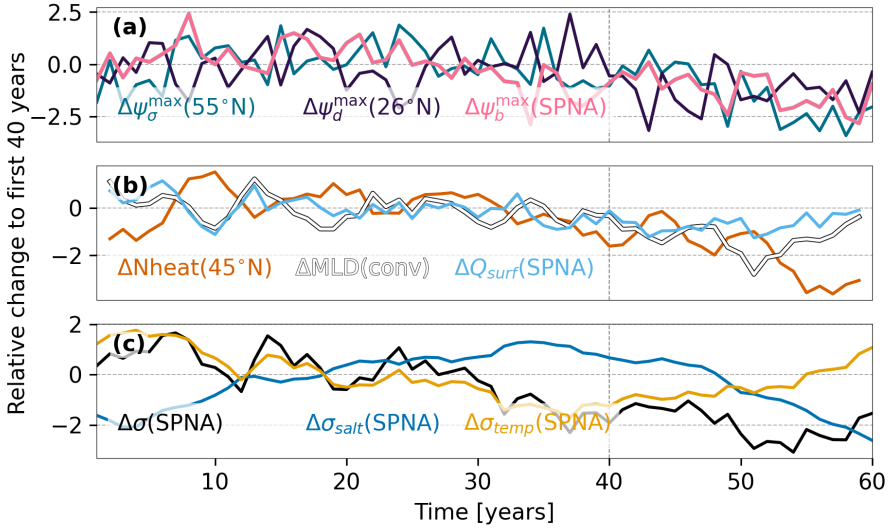

Figure 7. Same as Fig. 4 but here for 2σ decrease shifts before 1985.

ciated overturning fall well below the mean of the first 40 years. At year 50 the density trend is driven chiefly by declining salinity; convection has weakened markedly, and horizontal transport and overturning continue to subside. In the final years of the composite period cooling begins to offset the freshening-induced density reduction, which leads to stopping the decline in density overturning (Fig. 7a and c).

3.3 Post–1985 shifts towards decreased overturning

We examine the post–1985 weakening shifts separately because their evolution and spatial patterns differ from those of the pre–1985 period. Shortly before the shift, warming of the upper 500 m across the whole North Atlantic basin is evident (Fig. 8e). In year 39 a spike in northward heat transport coincides with a temporary reduction in surface heat loss that lowers temperature-driven density in the SPNA (Fig. 9c). The combination of basin-wide warming and reduced heat loss enhances stratification (Fig. 5i–l), suppresses convection, and weakens density overturning.

The strong surface forcing together with reduced density overturning alters density throughout the SPNA (Fig. 9)c. The resulting suppression of vertical mixing causes a density decrease across the upper 1000 m of the basin (Fig. 5i–l). Within a few years the thermal perturbation propagates downward: the deepest part of the anomaly first appears in the Irminger and Labrador Seas, where it spans the full water column. Within five years the deep signal has recirculated into the other two sections (Fig. 5i–l). The reduced convection consequently also weakens SPG strength (Fig. 8b and c).

With density and depth overturning decreasing, northward transport at ∼45° N also declines (Fig. 9a and b). Although surface heat flux diminishes, temperature within the SPG rises, with the temperature component of density reaching its minimum at year 45, marking the onset of SPG cooling. Reduced overturning and weakened inter-gyre exchange curtail northward heat and salt

https://doi.org/10.5194/egusphere-2026-2588
Preprint. Discussion started: 20 May 2026

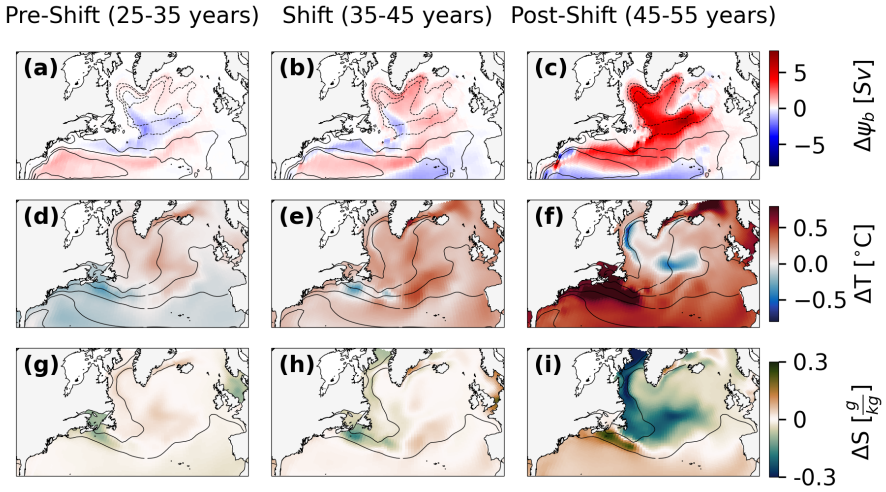

Figure 8. Same as Fig. 3 but here for 3σ decrease shifts after 1985.

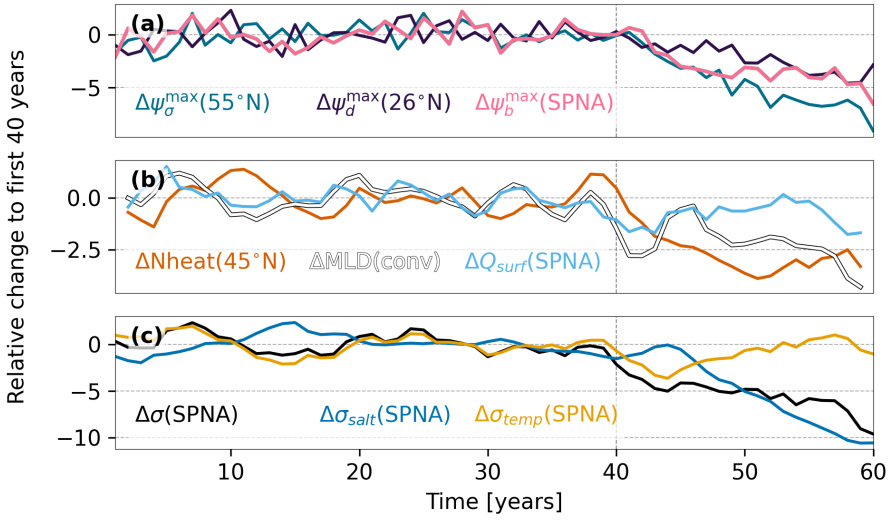

Figure 9. Same as Fig. 4 but here for3σ decrease shifts after 1985.

transport. The resultant cooling moderates the density decrease in the SPG, whereas the STG continues to warm, particularly south of the Grand Banks, where horizontal transport remains robust and the North Atlantic current shifts northward (Fig. 5i–l, Fig. 8, Fig. 9). Across the SPNA, salinity-driven density reductions persist, suppressing convection and further weakening both density overturning and horizontal transport.

https://doi.org/10.5194/egusphere-2026-2588
Preprint. Discussion started: 20 May 2026

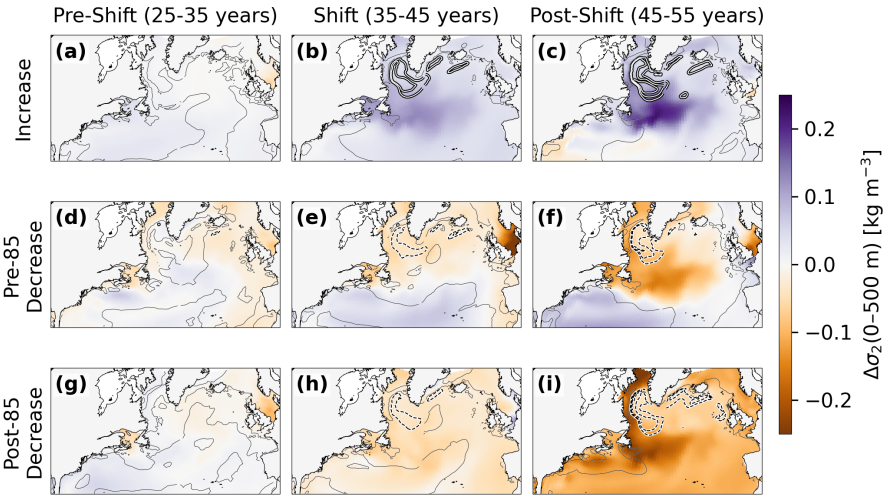

Figure 10. Ten-year averaged composites of 0–500 m potential density anomalies ($\Delta\sigma_2$, kg m^{-3}) using a PuOr colour scale. Rows represent: increase shifts **(a–c)**, pre-1985 decreases **(d–f)**, and post-1985 decreases **(g–i)**. The contours show MLD anomalies plotted every 50 m; solid lines indicate positive and dash-dot lines indicate negative anomalies.

3.4 Comparison of mechanisms driving abrupt changes in density overturning

A comparison of the three mechanisms reveals asymmetries in their timing and underlying processes. For this, upper-500 m density anomalies and mixed layer depth changes are shown in Fig. 10, synthesising the contrasting patterns across the three mechanisms.

During increases in density overturning, our results are consistent with a positive feedback between surface heat loss, deep convection, and horizontal transport within the SPG. The simultaneous intensification of overturning drives greater northward heat and salt transport into the gyre, initially causing further reinforcement of this feedback and promoting the southward expansion of the SPG. Over time, accumulated heat reduces density and weakens convection, providing a delayed negative feedback that ends the strengthening phase.

In the pre–1985 decreases, SPG warming and the associated lowering of density in the region induce the initial reduction in horizontal and northward heat transport. This weakens the density gradient between the SPG and STG, a positive feedback that further suppresses northward heat transport across 45°N and deep convection, with the largest reductions in the Labrador Sea. The resulting SPNA-wide cooling initiates the recovery of overturning.

In the post–1985 decreases, basin-wide surface warming precedes the shift. This warming is coupled with reductions in surface heat loss, convection, horizontal advection, and northward heat transport, a positive feedback that decreases overturning strength. Convection declines in the Labrador Sea, with marked reductions also in the Irminger Sea and eastern subpolar North Atlantic. The SPG's southward extent contracts, and it cools and freshens, with the resulting salinity deficit preventing overturning restoration.

https://doi.org/10.5194/egusphere-2026-2588
Preprint. Discussion started: 20 May 2026

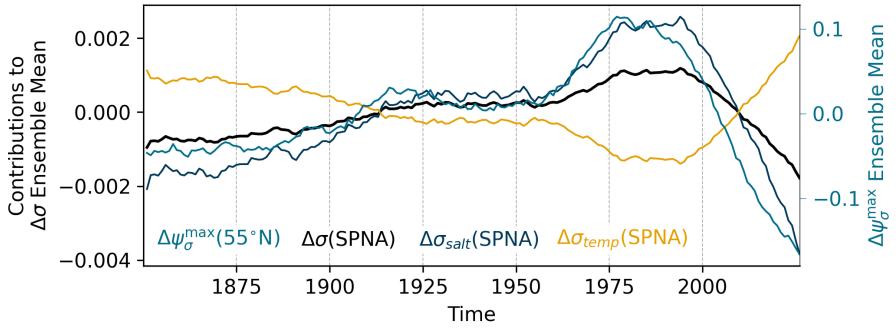

Figure 11. Normalised anomalies of density overturning strength at 55°N ($\Delta\psi_\sigma^{\max}$, green), SPNA density ($\Delta\sigma(\mathrm{SPNA})$; black), thermal contribution to density ($\Delta\sigma_{temp}(\mathrm{SPNA})$; yellow), haline contribution to density ($\Delta\sigma_{salt}(\mathrm{SPNA})$; blue), from 1850 to 2025. Values are expressed as deviations from the mean over the period 1980 to 2025, relative to that mean.

In summary, during shifts towards increased overturning, density within the SPG rises during the shift and intensifies thereafter, coinciding with southward expansion of the gyre. In pre–1985 decreases, density declines in the SPG and increases in the STG, reflecting a reduced meridional inter-gyre density gradient. Post–1985 decreases exhibit a basin-wide density decline in both the SPG and STG. Convection reductions in the pre–1985 events are largely confined to the Labrador Sea, whereas post–1985 events also display strong declines in the Irminger Sea and eastern subpolar North Atlantic. Given the mechanisms evolve differently, neither the pre- or post- 1985 decrease events represent a linear, symmetric counterpart to the increase shift; instead, non-linear processes govern the dynamics of these circulation shifts.

3.5 Abrupt shifts and historical trends

The abrupt circulation shifts identified here (Fig. 2) are intrinsically linked to long-term historical trends, reflecting not only the evolving overturning strength but also gradual changes in SPNA water column density and its constituent thermal and haline components (Fig. 11).

Two distinct periods of strengthening shifts occur within the historical record (Fig. 2). During these intervals, although the thermal contribution to density declines, consistent with SPG warming, the haline contribution increases sufficiently to drive an overall rise in total density (Fig. 11). This indicates that salinity changes exert primary control over density during these shifts, as total density variations track the haline component more closely than the thermal one. The concurrent strengthening of density overturning and associated salinification align with the positive feedback between transport and salinity described earlier.

The period associated with pre–1985 decrease shifts is characterised by stable ensemble-mean density and a slight reduction in density overturning. This is followed by a phase dominated by increase shifts, during which total density rises. In contrast, the conditions preceding post–1985 weakening shifts emerge around 1975, at a time when total density is already high due to the dominant influence of the haline contribution. The decline in overturning strength at 55° N leads the full-depth density

https://doi.org/10.5194/egusphere-2026-2588
Preprint. Discussion started: 20 May 2026

signal, reflecting the immediate impact of surface-driven processes on circulation before they manifest in the integrated water column. This timing is consistent with our composite analysis, where an initial peak in in northward heat transport introduces warmer subtropical water into the gyre, triggering the circulation shift which then leads to the broader density decline. Around 2000, when most decrease shifts occur, the haline contribution in the ensemble mean declines while the thermal contribution increases, reflecting SPG cooling. Total density subsequently falls sharply. Ultimately, these distinctions reveal a fundamental regime change in North Atlantic dynamics, where the mechanisms driving abrupt circulation shifts transition from internal density-gradient adjustments to a forced, basin-wide thermodynamic regime change.

4 Discussion and conclusions

In this study, we carried out a composite analysis using a 100-member ensemble to investigate abrupt shifts in density overturning strength at 55° N and to identify the underlying processes driving these shifts. We categorised the shifts into three distinct types: increases, decreases before 1985, and decreases after 1985. Increase events are sustained by an internal positive feedback where strengthened overturning enhances northward heat and salt transport into the SPG. In pre–1985 decreases, warming of the gyre reduces its density relative to the subtropics, weakening the meridional gradient and further suppressing overturning. Post–1985 decreases are reinforced by a basin-wide warming that coincides with reduced surface forcing, leading to persistent freshening of the gyre and continued weakening.

For increase events, our results show that an increase in surface heat loss in the central SPG coincides with a rise in upper-ocean density, reducing stratification and thereby enhancing deep convection. This pattern is consistent with Labrador Sea observations by Lazier et al. (2002), who reported intensified convection when surface cooling exceeded the horizontal heat flux. Enhanced deep convection, captured in the composites, precedes the strengthening of the baroclinic flow of relatively light water around the dense SPG centre. This forms a positive feedback mechanism between convection and horizontal transport that has been previously described by Born and Mignot (2012). However, of the current CMIP models, only CESM2 shows unambiguous signs of this process (Falkena et al., 2025). Our results show that increased northward heat transport into the SPG is offset by enhanced surface heat loss, preventing immediate warming. Instead, the accompanying salinity increase raises upper-ocean density, sustaining the strengthening of the overturning circulation, consistent with Moat et al. (2019), who identified meridional ocean heat transport as a key control on subpolar gyre dynamics and observed sea surface temperature changes preceding deeper-ocean heat content anomalies in HadGEM3–GC2.

We find that the upper-ocean temperature anomaly pattern of the pre–1985 decrease shifts resembles the Atlantic Multidecadal Variability (AMV) horseshoe pattern described by Zhang et al. (2019) for the positive phase of the AMV, which coincides with the period of these shifts. For the case of these $2\,\sigma$ shifts, the pattern is accompanied by additional cooling in the north-western STG, which strengthens the meridional density feedback and weakens the density gradient between the SPG and STG. This amplifies the reduction in overturning and appears to underlie the occurrence of the extreme shifts.

Convection reductions in the pre–1985 decreases are largely confined to the Labrador Sea. In contrast, the post–1985 decreases show strong declines extending into the Irminger Sea and eastern SPNA. This post–1985 pattern is consistent with

https://doi.org/10.5194/egusphere-2026-2588
Preprint. Discussion started: 20 May 2026

observational findings by Rühs et al. (2021), who reported an eastward shift of deep convection in the 21st century, increasing the relative importance of the Irminger Sea. These post–1985 changes form part of the third mechanism, in which warmer SSTs and reduced surface heat loss increase thermal buoyancy across the SPNA. across the SPNA. Convection weakens and density decreases throughout the water column, reflecting the positive feedback described by Megann et al. (2021), where subpolar SST changes reduce buoyancy losses and sustain AMOC decline. We also find that convection and surface heat loss are not as closely aligned in post–1985 decreases, a feature that has been identified by Rühs et al. (2021), who suggested that this decoupling could be linked to increased freshwater input from Greenland.

Density anomaly propagation is a mechanism that modulates multidecadal North Atlantic variability by connecting buoyancy forcing to circulation responses. Our results show the SPG acts as a conduit for these signals, consistent with Wills et al. (2019). As described by Eden and Willebrand (2001), the baroclinic response allows density anomalies to propagate across the basin and penetrate the deep ocean. This is evident in our tracking of anomalies in the Labrador and Irminger Seas (Fig. 5), where vertical propagation anchors the circulation changes. These patterns match the anticlockwise heat content propagation described by Moat et al. (2019) and the coupling between deep flows and gyre circulation noted by Kwon and Frankignoul (2014).

The role of the western SPG margin as a pacemaker for overturning (Tulloch and Marshall, 2012) is reflected in our circulation shifts, where inter-gyre exchange plays a defining role. Figure 11 shows that characterising upper-ocean density anomalies captures the key phenomena and contrasts underlying these multidecadal shifts. Complementary analysis of temperature and salinity, alongside density evolution with depth and its decomposition, further clarifies the mechanisms of anomaly origin, propagation, and overturning feedbacks. While buoyancy forcing in the western SPG triggers west-to-east propagation (Yeager et al., 2012), the resulting shifts are driven by the specific interplay between these thermal and haline signals. These shifts are consistent with established oceanographic principles, though the 1° resolution may not fully capture the boundary processes involved in their initiation. Future research using high-resolution simulations could further clarify how eddies and narrow currents modulate the density propagation and inter-gyre exchange identified here.

This study examines the historical period, during which anthropogenic forcing plays a central role in shaping North Atlantic dynamics and influencing how the overturning system responds to variability. Already in 2012, Booth et al. (2012) showed that anthropogenic aerosols were a major driver of North Atlantic climate variability, with aerosol–cloud microphysical effects dominating the magnitude and spatial pattern of forcing. Menary et al. (2020) linked the CMIP6 AMOC peak in the 1980s to prior aerosol-driven strengthening associated with rising global aerosol optical depth; they describe how, when aerosol emissions levelled off, greenhouse gas-driven AMOC decline took over. Robson et al. (2022) describe how, in CMIP6 historical simulations, aerosol forcing strengthens the AMOC through enhanced turbulent heat loss in the SPNA. This process feeds back positively via warmer SPNA sea surface temperatures that further raise turbulent heat loss and increased surface density from greater northward transport of saline waters—mechanisms closely resembling those we find for increase shifts in our study. Despite these physical consistencies, CMIP6 models may be more sensitive to aerosol forcing than observations suggest (Hassan et al., 2021), though effective radiative forcing estimates are broadly consistent across models and empirical data. Moreover, the CMIP6-simulated increase in AMOC during much of the historical period, peaking in the 1980s (Weijer et al., 2020), is not

https://doi.org/10.5194/egusphere-2026-2588
Preprint. Discussion started: 20 May 2026

uniformly supported by observational records. CESM2 shares these discrepancies, highlighting that the mechanisms identified here, while coherent within the model framework, may not fully represent real-world behaviour and should be tested against observational datasets across multiple timescales.

Our findings indicate a regime shift in large-scale SPG circulation linked to changes in the balance between aerosol and greenhouse gas forcing, with a corresponding change in the mechanisms driving these dynamics. We find that the relative contributions of salinity-driven density increases and temperature-driven density changes are critical in determining both the initiation and the persistence of such shifts. Given that the SPG has undergone abrupt transitions in the past (Li and Born, 2019), the possibility of similar or more intense circulation changes in the future warrants serious attention. In a related study, Swingedouw et al. (2021) identified abrupt SPG cooling events in four of 35 CMIP6 future projections, pointing to a non-negligible risk of rapid circulation changes in state-of-the-art climate models. Such potential instability reinforces the urgency of rapid and effective reductions in global greenhouse gas emissions to prevent continued alteration of AMOC control parameters (Ditlevsen and Ditlevsen, 2023). Given evidence that even modest warming may trigger catastrophic climate outcomes (Kemp et al., 2022), it is critical to broaden research to assess extreme risks, including cascades and systemic impacts, to support robust decision-making. Continued anthropogenic pressures on the Earth system could disrupt established circulation patterns in both ocean and atmosphere (Loriani et al., 2025), underscoring the need to confront the forces that entrench high-emission trajectories and to reimagine the social, economic, and political structures that shape our collective response to the climate crisis (Stoddard et al., 2021).

Code and data availability. The analysis code used in this study is publicly available at https://doi.org/10.5281/zenodo.19979604. The data for this study come from the CESM2 Large Ensemble Community Project and supercomputing resources provided by the IBS Center for Climate Physics in South Korea, and can be found via https://doi.org/10.5194/esd-12-1393-2021

Author contributions. IN performed the change point and composite analyses, generated all figures, and wrote the manuscript. HA and LB contributed ideas to the analysis, helped refine the methodology, and contributed to the text.

Competing interests. The author declares that there are no competing interests.

Acknowledgements. The author thanks the National Center for Atmospheric Research (NCAR) for providing the CESM2 Large Ensemble data. The data analysis was performed using the computing and storage resources provided by the Bjerknes Centre for Climate Research (BCCR). IN was supported by the BCCR strategic project DYNASOR. HA was supported by the Norwegian Research Council project GYRED (grant 352418).

https://doi.org/10.5194/egusphere-2026-2588
Preprint. Discussion started: 20 May 2026

References

Asbjørnsen, H., Johnson, H. L., and Årthun, M.: Variable Nordic Seas Inflow Linked to Shifts in North Atlantic Circulation, J. Climate, pp. 1–50, https://doi.org/10.1175/JCLI-D-20-0917.1, 2021.

Bellomo, K., Murphy, L. N., Cane, M. A., Clement, A. C., and Polvani, L. M.: Historical Forcings as Main Drivers of the Atlantic Multi-
345 decadal Variability in the CESM Large Ensemble, Clim. Dynam., 50, 3687–3698, https://doi.org/10.1007/s00382-017-3834-3, 2018.

Berglund, S., Döös, K., Groeskamp, S., and McDougall, T.: North Atlantic Ocean Circulation and Related Exchange of Heat and Salt Between Water Masses, Geophys. Res. Lett., 50, e2022GL100 989, https://doi.org/10.1029/2022GL100989, 2023.

Booth, B. B. B., Dunstone, N. J., Halloran, P. R., Andrews, T., and Bellouin, N.: Aerosols Implicated as a Prime Driver of Twentieth-Century North Atlantic Climate Variability, Nature, 484, 228–232, https://doi.org/10.1038/nature10946, 2012.

350 Born, A. and Mignot, J.: Dynamics of Decadal Variability in the Atlantic Subpolar Gyre: A Stochastically Forced Oscillator, Clim. Dynam., 39, 461–474, https://doi.org/10.1007/s00382-011-1180-4, 2012.

Born, A., Stocker, T. F., Raible, C. C., and Levermann, A.: Is the Atlantic Subpolar Gyre Bistable in Comprehensive Coupled Climate Models?, Clim. Dynam., 40, 2993–3007, https://doi.org/10.1007/s00382-012-1525-7, 2013.

Calvin, K., Dasgupta, D., Krinner, G., Mukherji, A., Thorne, P. W., Trisos, C., Romero, J., Aldunce, P., Barrett, K., Blanco, G., Cheung, W. W.,
355 Connors, S., Denton, F., Diongue-Niang, A., Dodman, D., Garschagen, M., Geden, O., Hayward, B., Jones, C., Jotzo, F., Krug, T., Lasco, R., Lee, Y.-Y., Masson-Delmotte, V., Meinshausen, M., Mintenbeck, K., Mokssit, A., Otto, F. E., Pathak, M., Pirani, A., Poloczanska, E., Pörtner, H.-O., Revi, A., Roberts, D. C., Roy, J., Ruane, A. C., Skea, J., Shukla, P. R., Slade, R., Slangen, A., Sokona, Y., Sörensson, A. A., Tignor, M., Van Vuuren, D., Wei, Y.-M., Winkler, H., Zhai, P., Zommers, Z., Hourcade, J.-C., Johnson, F. X., Pachauri, S., Simpson, N. P., Singh, C., Thomas, A., Totin, E., Arias, P., Bustamante, M., Elgizouli, I., Flato, G., Howden, M., Méndez-Vallejo, C., Pereira, J. J.,
360 Pichs-Madruga, R., Rose, S. K., Saheb, Y., Sánchez Rodríguez, R., Ürge-Vorsatz, D., Xiao, C., Yassaa, N., Alegría, A., Armour, K., Bednar-Friedl, B., Blok, K., Cissé, G., Dentener, F., Eriksen, S., Fischer, E., Garner, G., Guivarch, C., Haasnoot, M., Hansen, G., Hauser, M., Hawkins, E., Hermans, T., Kopp, R., Leprince-Ringuet, N., Lewis, J., Ley, D., Ludden, C., Niamir, L., Nicholls, Z., Some, S., Szopa, S., Trewin, B., Van Der Wijst, K.-I., Winter, G., Witting, M., Birt, A., Ha, M., Romero, J., Kim, J., Haites, E. F., Jung, Y., Stavins, R., Birt, A., Ha, M., Orendain, D. J. A., Ignon, L., Park, S., Park, Y., Reisinger, A., Cammaramo, D., Fischlin, A., Fuglestvedt, J. S., Hansen,
365 G., Ludden, C., Masson-Delmotte, V., Matthews, J. R., Mintenbeck, K., Pirani, A., Poloczanska, E., Leprince-Ringuet, N., and Péan, C.: IPCC, 2023: Climate Change 2023: Synthesis Report. Contribution of Working Groups I, II and III to the Sixth Assessment Report of the Intergovernmental Panel on Climate Change [Core Writing Team, H. Lee and J. Romero (Eds.)]. IPCC, Geneva, Switzerland., Tech. rep., Intergovernmental Panel on Climate Change (IPCC), https://doi.org/10.59327/IPCC/AR6-9789291691647, 2023.

Danabasoglu, G.: On Multidecadal Variability of the Atlantic Meridional Overturning Circulation in the Community Climate System Model
370 Version 3, Journal of Climate, 21, 5524–5544, https://doi.org/10.1175/2008JCLI2019.1, 2008.

Danabasoglu, G., Lamarque, J.-F., Bacmeister, J., Bailey, D. A., DuVivier, A. K., Edwards, J., Emmons, L. K., Fasullo, J., Garcia, R., Gettelman, A., Hannay, C., Holland, M. M., Large, W. G., Lauritzen, P. H., Lawrence, D. M., Lenaerts, J. T. M., Lindsay, K., Lipscomb, W. H., Mills, M. J., Neale, R., Oleson, K. W., Otto-Bliesner, B., Phillips, A. S., Sacks, W., Tilmes, S., Kampenhout, L., Vertenstein, M., Bertini, A., Dennis, J., Deser, C., Fischer, C., Fox-Kemper, B., Kay, J. E., Kinnison, D., Kushner, P. J., Larson, V. E., Long, M. C.,
375 Mickelson, S., Moore, J. K., Nienhouse, E., Polvani, L., Rasch, P. J., and Strand, W. G.: The Community Earth System Model Version 2 (CESM2), J. Adv. Model. Earth Syst., 12, https://doi.org/10.1029/2019MS001916, 2020.

https://doi.org/10.5194/egusphere-2026-2588
Preprint. Discussion started: 20 May 2026

Dey, D., Marsh, R., Drijfhout, S., Josey, S. A., Sinha, B., Grist, J., and Döös, K.: Formation of the Atlantic Meridional Overturning Circulation Lower Limb Is Critically Dependent on Atlantic-Arctic Mixing, Nat. Commun., 15, https://doi.org/10.1038/s41467-024-51777-w, 2024.

Dickson, R. R., Meincke, J., Malmberg, S.-A., and Lee, A. J.: The "Great Salinity Anomaly" in the Northern North Atlantic 1968–1982, Prog. Oceanogr., 20, 103–151, https://doi.org/10.1016/0079-6611(88)90049-3, 1988.

Ditlevsen, P. and Ditlevsen, S.: Warning of a Forthcoming Collapse of the Atlantic Meridional Overturning Circulation, Nat. Commun., 14, 4254, https://doi.org/10.1038/s41467-023-39810-w, 2023.

Eden, C. and Willebrand, J.: Mechanism of Interannual to Decadal Variability of the North Atlantic Circulation, Journal of Climate, 14, 2266–2280, https://doi.org/10.1175/1520-0442(2001)014<2266:MOITDV>2.0.CO;2, 2001.

Evans, D. G., Holliday, N. P., Bacon, S., and Le Bras, I.: Mixing and Air–Sea Buoyancy Fluxes Set the Time-Mean Overturning Circulation in the Subpolar North Atlantic and Nordic Seas, Ocean Sci., 19, 745–768, https://doi.org/10.5194/os-19-745-2023, 2023.

Falkena, S. K. J., Dijkstra, H. A., and Von Der Heydt, A. S.: Causal Mechanisms of Subpolar Gyre Variability in CMIP6 Models, Earth Syst. Dynam., 16, 1833–1844, https://doi.org/10.5194/esd-16-1833-2025, 2025.

Fox-Kemper, B., Hewitt, H. T., Xiao, C., Aðalgeirsdóttir, G., Drijfhout, S. S., Tamsin L. Edwards, Nicholas R. Golledge, Mark Hemer, Robert E. Kopp, Gerhard Krinner, Alan Mix, Dirk Notz, Sophie Nowicki, Intan Suci Nurhati, Lucas Ruiz, Jean-Baptiste Sallé, Aimee B.A. Slangen, and Yongqiang Yu: Ocean, Cryosphere and Sea Level Change, Climate Change 2021: The Physical Science Basis. Contribution of Working Group I to the Sixth Assessment Report of the Intergovernmental Panel on Climate Change, pp. 1211–1362, 2021.

Gu, Q., Gervais, M., Danabasoglu, G., Kim, W. M., Castruccio, F., Maroon, E., and Xie, S.-P.: Wide Range of Possible Trajectories of North Atlantic Climate in a Warming World, Nat. Commun., 15, 4221, https://doi.org/10.1038/s41467-024-48401-2, 2024.

Hassan, T., Allen, R. J., Liu, W., and Randles, C. A.: Anthropogenic Aerosol Forcing of the Atlantic Meridional Overturning Circulation and the Associated Mechanisms in CMIP6 Models, Atmos. Chem. Phys., 21, 5821–5846, https://doi.org/10.5194/acp-21-5821-2021, 2021.

Holliday, N. P., Bersch, M., Berx, B., Chafik, L., Cunningham, S., Florindo-López, C., Hátún, H., Johns, W., Josey, S. A., Larsen, K. M. H., Mulet, S., Oltmanns, M., Reverdin, G., Rossby, T., Thierry, V., Valdimarsson, H., and Yashayaev, I.: Ocean Circulation Causes the Largest Freshening Event for 120 Years in Eastern Subpolar North Atlantic, Nat. Commun., 11, 585, https://doi.org/10.1038/s41467-020-14474-y, 2020.

Kemp, L., Xu, C., Depledge, J., Ebi, K. L., Gibbins, G., Kohler, T. A., Rockström, J., Scheffer, M., Schellnhuber, H. J., Steffen, W., and Lenton, T. M.: Climate Endgame: Exploring Catastrophic Climate Change Scenarios, Proc. Natl. Acad. Sci. U.S.A., 119, e2108146 119, https://doi.org/10.1073/pnas.2108146119, 2022.

Kostov, Y., Johnson, H. L., Marshall, D. P., Heimbach, P., Forget, G., Holliday, N. P., Lozier, M. S., Li, F., Pillar, H. R., and Smith, T.: Distinct Sources of Interannual Subtropical and Subpolar Atlantic Overturning Variability, Nat. Geosci., 14, 491–495, https://doi.org/10.1038/s41561-021-00759-4, 2021.

Kwon, Y.-O. and Frankignoul, C.: Mechanisms of Multidecadal Atlantic Meridional Overturning Circulation Variability Diagnosed in Depth versus Density Space, Journal of Climate, 27, 9359–9376, https://doi.org/10.1175/JCLI-D-14-00228.1, 2014.

Lai, W. K. M., Robson, J. I., Wilcox, L. J., and Dunstone, N.: Mechanisms of Internal Atlantic Multidecadal Variability in HadGEM3-GC3.1 at Two Different Resolutions, Journal of Climate, 35, 1365–1383, https://doi.org/10.1175/jcli-d-21-0281.1, 2022.

Latif, M., Sun, J., Visbeck, M., and Hadi Bordbar, M.: Natural Variability Has Dominated Atlantic Meridional Overturning Circulation since 1900, Nat. Clim. Chang., 12, 455–460, https://doi.org/10.1038/s41558-022-01342-4, 2022.

Lazier, J., Hendry, R., Clarke, A., Yashayaev, I., and Rhines, P.: Convection and Restratification in the Labrador Sea, 1990–2000, Deep-Sea Res. Pt. I, 49, 1819–1835, https://doi.org/10.1016/S0967-0637(02)00064-X, 2002.

https://doi.org/10.5194/egusphere-2026-2588
Preprint. Discussion started: 20 May 2026

Li, C. and Born, A.: Coupled Atmosphere-Ice-Ocean Dynamics in Dansgaard-Oeschger Events, Quat. Sci. Rev., 203, 1–20, https://doi.org/10.1016/j.quascirev.2018.10.031, 2019.

Lohmann, K., Drange, H., and Bentsen, M.: Response of the North Atlantic Subpolar Gyre to Persistent North Atlantic Oscillation like Forcing, Clim. Dynam., 32, 273–285, https://doi.org/10.1007/s00382-008-0467-6, 2009.

Loriani, S., Aksenov, Y., Armstrong McKay, D. I., Bala, G., Born, A., Chiessi, C. M., Dijkstra, H. A., Donges, J. F., Drijfhout, S., England, M. H., Fedorov, A. V., Jackson, L. C., Kornhuber, K., Messori, G., Pausata, F. S. R., Rynders, S., Sallée, J.-B., Sinha, B., Sherwood, S. C., Swingedouw, D., and Tharammal, T.: Tipping Points in Ocean and Atmosphere Circulations, Earth Syst. Dynam., 16, 1611–1653, https://doi.org/10.5194/esd-16-1611-2025, 2025.

Lozier, M. S.: Deconstructing the Conveyor Belt, Science, 328, 1507–1511, https://doi.org/10.1126/science.1189250, 2010.

Lozier, M. S.: Overturning in the Subpolar North Atlantic: A Review, Phil. Trans. R. Soc. A., 381, 20220 191, https://doi.org/10.1098/rsta.2022.0191, 2023.

Lozier, M. S., Li, F., Bacon, S., Bahr, F., Bower, A. S., Cunningham, S. A., de Jong, M. F., de Steur, L., deYoung, B., Fischer, J., Gary, S. F., Greenan, B. J. W., Holliday, N. P., Houk, A., Houpert, L., Inall, M. E., Johns, W. E., Johnson, H. L., Johnson, C., Karstensen, J., Koman, G., Le Bras, I. A., Lin, X., Mackay, N., Marshall, D. P., Mercier, H., Oltmanns, M., Pickart, R. S., Ramsey, A. L., Rayner, D., Straneo, F., Thierry, V., Torres, D. J., Williams, R. G., Wilson, C., Yang, J., Yashayaev, I., and Zhao, J.: A Sea Change in Our View of Overturning in the Subpolar North Atlantic, Science, 363, 516–521, https://doi.org/10.1126/science.aau6592, 2019.

Megann, A., Blaker, A., Josey, S., New, A., and Sinha, B.: Mechanisms for Late 20th and Early 21st Century Decadal AMOC Variability, J. Geophys. Res. Oceans, 126, e2021JC017 865, https://doi.org/10.1029/2021JC017865, 2021.

Menary, M. B., Robson, J., Allan, R. P., Booth, B. B. B., Cassou, C., Gastineau, G., Gregory, J., Hodson, D., Jones, C., Mignot, J., Ringer, M., Sutton, R., Wilcox, L., and Zhang, R.: Aerosol-Forced AMOC Changes in CMIP6 Historical Simulations, Geophys. Res. Lett., 47, e2020GL088 166, https://doi.org/10.1029/2020GL088166, 2020.

Moat, B. I., Sinha, B., Josey, S. A., Robson, J., Ortega, P., Sévellec, F., Holliday, N. P., McCarthy, G. D., New, A. L., and Hirschi, J. J.-M.: Insights into Decadal North Atlantic Sea Surface Temperature and Ocean Heat Content Variability from an Eddy-Permitting Coupled Climate Model, Journal of Climate, 32, 6137–6161, https://doi.org/10.1175/JCLI-D-18-0709.1, 2019.

Moat, B. I., Sinha, B., Berry, D. I., Drijfhout, S. S., Fraser, N., Hermanson, L., Jones, D. C., Josey, S. A., King, B., Macintosh, C., Megann, A., Oltmanns, M., Sanders, R., and Williams, S.: Ocean Heat Convergence and North Atlantic Multidecadal Heat Content Variability, Journal of Climate, 37, 4723–4742, https://doi.org/10.1175/JCLI-D-23-0370.1, 2024.

Oliveira Matos, F. D. A., Sidorenko, D., Shi, X., Ackermann, L., Pereira, J., Lohmann, G., and Stepanek, C.: Diagnosing the Atlantic Meridional Overturning Circulation in Density Space Is Critical in Warmer Climates, Ocean Sci., 21, 2895–2914, https://doi.org/10.5194/os-21-2895-2025, 2025.

Rhein, M., Kieke, D., and Steinfeldt, R.: Advection of North Atlantic Deep Water from the Labrador Sea to the Southern Hemisphere, J. Geophys. Res. Oceans, 120, 2471–2487, https://doi.org/10.1002/2014JC010605, 2015.

Robson, J., Sutton, R., Lohmann, K., Smith, D., and Palmer, M. D.: Causes of the Rapid Warming of the North Atlantic Ocean in the Mid-1990s, J. Climate, 25, 2012.

Robson, J., Sutton, R. T., Archibald, A., Cooper, F., Christensen, M., Gray, L. J., Holliday, N. P., Macintosh, C., McMillan, M., Moat, B., Russo, M., Tilling, R., Carslaw, K., Desbruyères, D., Embury, O., Feltham, D. L., Grosvenor, D. P., Josey, S., King, B., Lewis, A., McCarthy, G. D., Merchant, C., New, A. L., O'Reilly, C. H., Osprey, S. M., Read, K., Scaife, A., Shepherd, A., Sinha, B., Smeed, D.,

https://doi.org/10.5194/egusphere-2026-2588
Preprint. Discussion started: 20 May 2026

Smith, D., Ridout, A., Woollings, T., and Yang, M.: Recent Multivariate Changes in the North Atlantic Climate System, with a Focus on 2005–2016, Int. J. Climatol., 38, 5050–5076, https://doi.org/10.1002/joc.5815, 2018.

Robson, J., Menary, M. B., Sutton, R. T., Mecking, J., Gregory, J. M., Jones, C., Sinha, B., Stevens, D. P., and Wilcox, L. J.: The Role of Anthropogenic Aerosol Forcing in the 1850–1985 Strengthening of the AMOC in CMIP6 Historical Simulations, J. Climate, 35, 3243–3263, https://doi.org/10.1175/JCLI-D-22-0124.1, 2022.

Rodgers, K. B., Lee, S.-S., Rosenbloom, N., Timmermann, A., Danabasoglu, G., Deser, C., Edwards, J., Kim, J.-E., Simpson, I. R., Stein, K., Stuecker, M. F., Yamaguchi, R., Bódai, T., Chung, E.-S., Huang, L., Kim, W. M., Lamarque, J.-F., Lombardozzi, D. L., Wieder, W. R., and Yeager, S. G.: Ubiquity of Human-Induced Changes in Climate Variability, Earth Syst. Dynam., 12, 1393–1411, https://doi.org/10.5194/esd-12-1393-2021, 2021.

Rühs, S., Oliver, E. C. J., Biastoch, A., Böning, C. W., Dowd, M., Getzlaff, K., Martin, T., and Myers, P. G.: Changing Spatial Patterns of Deep Convection in the Subpolar North Atlantic, J. Geophys. Res. Oceans, 126, e2021JC017 245, https://doi.org/10.1029/2021JC017245, 2021.

Sévellec, F. and Huck, T.: Theoretical Investigation of the Atlantic Multidecadal Oscillation, Journal of Physical Oceanography, 45, 2189–2208, https://doi.org/10.1175/JPO-D-14-0094.1, 2015.

Stoddard, I., Anderson, K., Capstick, S., Carton, W., Depledge, J., Facer, K., Gough, C., Hache, F., Hoolohan, C., Hultman, M., Hällström, N., Kartha, S., Klinsky, S., Kuchler, M., Lövbrand, E., Nasiritousi, N., Newell, P., Peters, G. P., Sokona, Y., Stirling, A., Stilwell, M., Spash, C. L., and Williams, M.: Three Decades of Climate Mitigation: Why Haven't We Bent the Global Emissions Curve?, Annu. Rev. Environ. Resour., 46, 653–689, https://doi.org/10.1146/annurev-environ-012220-011104, 2021.

Sutton, R. T., McCarthy, G. D., Robson, J., Sinha, B., Archibald, A. T., and Gray, L. J.: Atlantic Multidecadal Variability and the U.K. ACSIS Program, Bulletin of the American Meteorological Society, 99, 415–425, https://doi.org/10.1175/BAMS-D-16-0266.1, 2018.

Swingedouw, D., Bily, A., Esquerdo, C., Borchert, L. F., Sgubin, G., Mignot, J., and Menary, M.: On the Risk of Abrupt Changes in the North Atlantic Subpolar Gyre in CMIP6 Models, Annals of the New York Academy of Sciences, 1504, 187–201, https://doi.org/10.1111/nyas.14659, 2021.

Te Raa, L. A. and Dijkstra, H. A.: Instability of the Thermohaline Ocean Circulation on Interdecadal Timescales, J. Phys. Oceanogr., 32, 138–160, https://doi.org/10.1175/1520-0485(2002)032<0138:IOTTOC>2.0.CO;2, 2002.

Truong, C., Oudre, L., and Vayatis, N.: Selective Review of Offline Change Point Detection Methods, Signal Process., 167, 107 299, https://doi.org/10.1016/j.sigpro.2019.107299, 2020.

Tulloch, R. and Marshall, J.: Exploring Mechanisms of Variability and Predictability of Atlantic Meridional Overturning Circulation in Two Coupled Climate Models, Journal of Climate, 25, 4067–4080, https://doi.org/10.1175/JCLI-D-11-00460.1, 2012.

Weijer, W., Cheng, W., Garuba, O. A., Hu, A., and Nadiga, B. T.: CMIP6 Models Predict Significant 21st Century Decline of the Atlantic Meridional Overturning Circulation, Geophys. Res. Lett., 47, e2019GL086 075, https://doi.org/10.1029/2019GL086075, 2020.

Wills, R. C. J., Armour, K. C., Battisti, D. S., and Hartmann, D. L.: Ocean–Atmosphere Dynamical Coupling Fundamental to the Atlantic Multidecadal Oscillation, Journal of Climate, 32, 251–272, https://doi.org/10.1175/jcli-d-18-0269.1, 2019.

Yeager, S. and Danabasoglu, G.: The Origins of Late-Twentieth-Century Variations in the Large-Scale North Atlantic Circulation, Journal of Climate, 27, 3222–3247, https://doi.org/10.1175/jcli-d-13-00125.1, 2014.

Yeager, S., Karspeck, A., Danabasoglu, G., Tribbia, J., and Teng, H.: A Decadal Prediction Case Study: Late Twentieth-Century North Atlantic Ocean Heat Content, Journal of Climate, 25, 5173–5189, https://doi.org/10.1175/JCLI-D-11-00595.1, 2012.

https://doi.org/10.5194/egusphere-2026-2588
Preprint. Discussion started: 20 May 2026

Yeager, S., Castruccio, F., Chang, P., Danabasoglu, G., Maroon, E., Small, J., Wang, H., Wu, L., and Zhang, S.: An Outsized Role for the Labrador Sea in the Multidecadal Variability of the Atlantic Overturning Circulation, Sci. Adv., 7, eabh3592, https://doi.org/10.1126/sciadv.abh3592, 2021.

Yeager, S. G. and Robson, J. I.: Recent Progress in Understanding and Predicting Atlantic Decadal Climate Variability, Curr. Clim. Change Rep., 3, 112–127, https://doi.org/10.1007/s40641-017-0064-z, 2017.

Zhang, J. and Zhang, R.: On the Evolution of Atlantic Meridional Overturning Circulation Fingerprint and Implications for Decadal Predictability in the North Atlantic, Geophysical Research Letters, 42, 5419–5426, https://doi.org/10.1002/2015gl064596, 2015.

Zhang, R.: Latitudinal Dependence of Atlantic Meridional Overturning Circulation (AMOC) Variations, Geophysical Research Letters, 37, https://doi.org/10.1029/2010gl044474, 2010.

Zhang, R., Sutton, R., Danabasoglu, G., Kwon, Y.-O., Marsh, R., Yeager, S. G., Amrhein, D. E., and Little, C. M.: A Review of the Role of the Atlantic Meridional Overturning Circulation in Atlantic Multidecadal Variability and Associated Climate Impacts, Rev. Geophys., 57, 316–375, https://doi.org/10.1029/2019RG000644, 2019.

Zhu, C., Liu, Z., Zhang, S., and Wu, L.: Likely Accelerated Weakening of Atlantic Overturning Circulation Emerges in Optimal Salinity Fingerprint, Nat. Commun., 14, 1245, https://doi.org/10.1038/s41467-023-36288-4, 2023.